

Radiographic and spectral images of rice seeds and the photosynthetic efficiency of seedlings

Artur Sousa Silva*^{ORCID}, Silvio Moure Cicero^{ORCID}, Francisco Guilhien Gomes Junior^{ORCID}

Universidade de São Paulo/ESALQ – Depto. de Produção Vegetal, C.P. 09 – 13418- 900 – Piracicaba, SP – Brasil.

*Corresponding author <artursilva.agro@gmail.com>

Edited by: Cesar Valmor Rombaldi/Jorge Alberto Marques Rezende

Received April 01, 2022

Accepted July 26, 2023

ABSTRACT: The development and the use of new technologies in agriculture contribute to significant advances in research with practical applications in several fields, such as image analytical techniques, which are simple, fast, and objective analyses. This work aimed to evaluate rice seeds' quality using X-ray, multispectral, and chlorophyll fluorescence image analytical techniques and relate this information with the photosynthetic efficiency of seedlings. Initially, the seeds were identified and enumerated, then X-ray images were obtained, and the void space (area between the endosperm + embryo and the glumes) was calculated. Next, the same seeds were used in the X-rays, multispectral, and chlorophyll fluorescence images. Afterward, the seeds were placed to germinate in polyethylene cups with a capacity of 250 mL, and evaluations of the photochemical yield of photosynthesis photosystem II (FSII) and of the seedling fluorescence chlorophyll were carried out seven, nine, and 11 days after the emergence of the seedlings. The reflectance of seeds in the spectral bands between 365 nm and 780 nm showed a positive correlation with the chlorophyll fluorescence. Furthermore, the higher photosynthetic efficiency of rice seedlings at 11 days after emergence is directly related to the reflectance of the seeds at spectral bands between 365 nm and 780 nm.

Keywords: X-ray, image analysis, multispectral images, chlorophyll fluorescence

Introduction

The occurrence of irregular flowering leads to uneven maturation of the seeds and grains, which is a major obstacle in rice crops. Thus, developing methods and machines to identify and dispose immature rice seeds accurately is highly desirable (Marcos-Filho et al., 2006).

The image analysis of seeds and seedlings has been used to assess seed quality of many species, with potential use in seed producing companies and seed analysis laboratories. In this sense, multispectral image (MSI) analyses are non-destructive, simple and fast, which allows their use online to monitor the production process and quality control of seeds (Olesen et al., 2011; Mastrangelo et al., 2019). This technology obtains spatial and spectral information from samples by combining computer vision and spectroscopy techniques, enabling the simultaneous measurement of several components related to seed quality (Shrestha et al., 2015; Boelt et al., 2018).

In addition to MSI, the chlorophyll fluorescence (CF) technique has become very relevant, as chlorophyll degradation typically occurs in the final stages of the seed maturation process (Smolikova et al., 2020; Smolikova et al., 2017 and the chlorophyll content and its fluorescence are inversely proportional to the seed maturation degree and, therefore, to its quality (Ooms and Destain, 2011).

The integrity of the photosynthetic apparatus of plants from green seeds is still unknown; however, these materials present irregular concentrations of chloroplast pigments and reactive oxygen species,

disrupting electron transport and the inactivation of enzymes and proteins (Ashraf and Harris, 2013; Mathur et al., 2014).

Seed maturation assessed by MSI techniques provides information on seed CF and photosystem II quantum yield, allowing for the joint data analysis that can be related to the physiological potential of seeds.

Considering image analysis techniques as alternatives for seed quality evaluation, this study aimed to assess the quality of rice seeds using X-ray, multispectral, and chlorophyll fluorescence image analysis techniques and relate this information to the photosynthetic efficiency of seedlings.

Materials and Methods

Seeds

The study was carried out using six batches of rice seeds, cultivar BRS Catiana, as it presents a high yield and a broad adaptation to all regions in Brazil. The batches were produced by Embrapa Rice and Beans (Empresa Brasileira de Pesquisa Agropecuária) in the 2017/2018 and 2018/2019 crop seasons.

The study was conducted in the municipality of Piracicaba, São Paulo State, Brazil, 22°43'30" S, 47°38'51" W, altitude 524 m.

Evaluation of the internal morphology of seeds

Four replicates of 20 seeds from each batch were used. The seeds were fixed with double-sided adhesive tape

in transparent Petri dishes measuring 9 cm in diameter, placing the seeds one by one and equidistant from each other under an identification sequence for subsequent tests to be carried out (Figure 1A). Radiographic images were obtained using the equipment MultiFocus Digital Radiography System (Faxitron Bioptics) for the evaluation of the internal morphology of the seeds. The radiographic images (Figure 1B) were saved in a specific folder on the computer hard drive connected to the X-ray equipment (Silva et al., 2023).

The radiographic images were analyzed using the software ImageJ, version 1.48v, to obtain the area of the internal free space of the seeds (Schneider et al., 2012), following the methodology proposed by Silva et al. (2013). The total area (mm²) and relative density (gray pixel⁻¹) of the individual seeds were also obtained.

Acquisition of multispectral and chlorophyll fluorescence images of seeds with a VideometerLab

After performing the X-ray test, also following the methodology proposed by Silva et al. (2023) for the acquisition and processing of images, each Petri dish containing the same seeds was placed under the integration sphere of the equipment VideometerLab4 (Videometer A/S) and, after successive activation of the 19 contiguous light-emitting diodes (LEDs) placed on the sphere edge, the standard monochromatic charge-coupled (CCD) chip recorded and captured the reflectance of the seeds, generating 19 spectral images corresponding to each length of the waveform (365, 405, 430, 450, 470, 490, 515, 540, 570, 590, 630, 645, 660, 690, 780, 850, 880, 940, 970 nm) per sample, with a resolution of 2056 × 2056 pixels (Figure 1C).

Three short optical density filters were added to measure the CF of the seeds, allowing the capture of radiation intensity only at a wavelength of 700 nm (emission energy), resulting in three specific images of the seeds, that is, bands corresponding to fluorescence for excitation energies of 630 nm (red region), 645 nm (chlorophyll *a*) and 660 nm (chlorophyll *b*).

Subsequently, the images were processed using the software VideometerLab4 version 3.14.9. The segmentation mask 'Blue background' was used for the segmentation of the background (Petri dish and noise) and the region of interest (seeds). Then, the seeds were selected individually using the 'full' command, providing the average reflectance of each seed and, from this, the CF and the other reflectance values of the corresponding spectrum bands were calculated.

The supervised method nCDA (Normalized Canonical Discriminant Analysis) was used to transform MSI to obtain seed color and texture parameters (Olesen et al., 2011). With the aid of the command "blob" (Binary Large Object), the seeds were analyzed individually and the color appearance attributes CIELab a* (green to red), CIELab b* (blue to yellow) and CIELab L (brightness of the glumes).

All data extracted from the multispectral images were exported to Excel.

Acquisition of chlorophyll *a* fluorescence images with the equipment SeedReporter

To obtain the CF images, the same seeds were transferred one by one to a polyethylene plate (11 × 11 × 0.5 cm) with concave cavities to accommodate the seeds, under the identification sequence. Then, the plates were placed inside the equipment integration cabin and the images were generated through the rapid repetition of the fluorometric rate (FRRF) and the duration of the pulses. Saturating subpulses that excite chlorophyll *a* were captured by a CCD camera. The chlorophyll excitation of the seeds was induced by the emission of radiation with a wavelength of 620 nm and the CF signals were detected at 730 nm, using a filter of this optical density. Images were generated in gray scale, with 320 × 240 pixels, synchronously within 4 s intervals (Figure 1D) (Silva et al., 2023).

The images were processed using the Data Analysis PhenoVation software (version 5.5.1). Each image was treated with filters to remove noise and a last filter to enable the CF reading of each seed, obtaining CF data of individual and sequenced seeds. The chlorophyll and anthocyanin indices were also obtained from the images.

Evaluation of photochemical yield of photosynthesis photosystem II (FSII) and seedling CF

To evaluate the photosynthetic efficiency, or the photochemical yield, of the photosynthesis photosystem II (FSII) of the seedlings, the seeds from the previous assessments (X-ray, multispectral and CF with the VideometerLab and SeedReporter equipment), were placed to germinate in a substrate consisting of a mixture of sand and earth at a 1:3 ratio, without fertilization, in polyethylene containers with a capacity of 250 mL. Then, the seeds were placed in a plant growth chamber at 25 °C and under constant lighting. Irrigation was carried out with a water volume equivalent to 60 % of the substrate holding capacity and, when necessary, additional irrigations were carried out to provide adequate water content to the substrate until the end of the evaluations.

At seven, nine, and 11 days after seedling emergence, the containers with seedlings from each batch were transferred to the laboratory and kept for 30 min in the dark. Then, the analyses were performed by the SeedReporter, obtaining the initial chlorophyll fluorescence (F_0) and the driving maximum fluorescence (F_m) (Figure 1E).

The quantum yield of the maximum photochemical efficiency of the FSII was calculated (F_v/F_m) based on the equation below, applied to each pixel:

$$\Phi_{po} = \frac{F_v}{F_m} = \frac{(F_m - F_0)}{F_m}$$

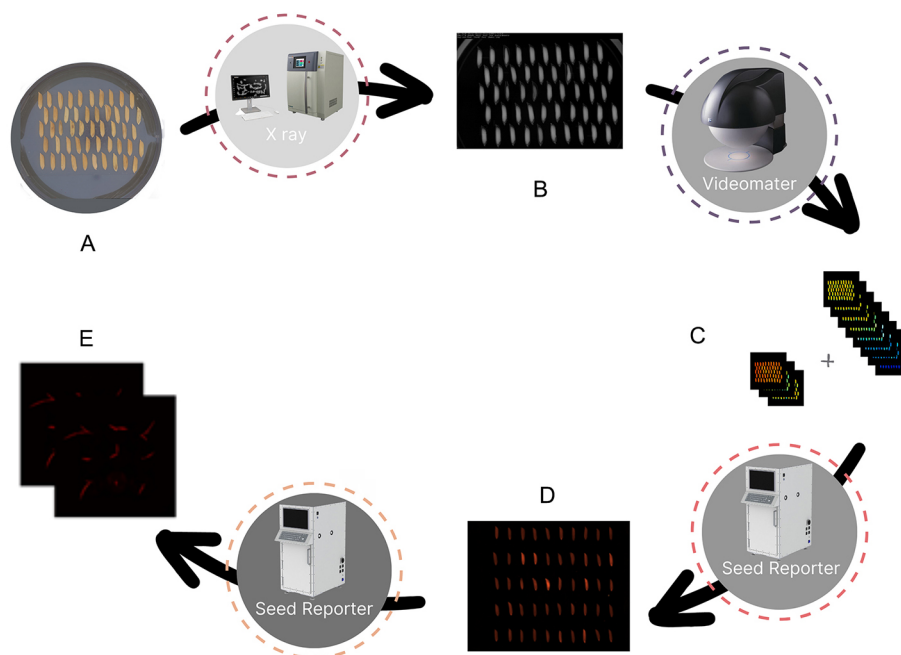


Figure 1 – Flowchart of the analyses performed: positioning the seeds of each repetition in Petri dishes (A); acquisition of X-ray images (B) and multispectral and chlorophyll fluorescence images with the VideometerLab equipment (C); obtaining chlorophyll a fluorescence images with the SeedReporter equipment (D); obtaining chlorophyll a fluorescence images, and the quantum yield of the FSII photochemical maximum efficiency (F_v/F_m) of the generated seedlings (E).

where: Φ_{po} and F_v/F_m are the maximum quantum yield of PSII and the maximum photochemical efficiency of FSII, respectively, and F_0 is the minimum fluorescence at time $t = 0$.

The chlorophyll index chlorophyll *a* was measured as described by Gitelson et al. (2003) based on reflectance from 710 nm to 770 nm, using the following formula:

$$Chl\ index = \left(\frac{\rho_{770}}{\rho_{710}} \right) - 1$$

where: ρ is the spectral reflectance for each wavelength.

Complementary physiological tests

Afterward, the seeds of these batches were evaluated for their physiological potential with the tests described below.

Germination test: carried out with four replications of 50 seeds in paper towel rolls moistened with an amount of water equivalent to 2.5 times the mass of dry paper in a germinator at 25 °C. The first and second counts were carried out five and 14 days after sowing, counting the percentage of normal seedlings (MAPA, 2009).

Accelerated aging test: four replications of 50 seeds were distributed in a single layer on a metallic screen suspended inside transparent plastic boxes (11 × 11 × 3 cm), containing 40 mL of distilled water at the bottom of the box. The boxes were kept at 41 °C for

96 h (AOSA, 2009). After this period, the germination test was installed, according to the previous item and the evaluation was carried out five days after the installation of the test. The results were expressed as a percentage of normal seedlings.

Seedling emergence test in the sand: four replications of 50 seeds were sown 1 cm deep in plastic boxes (32 × 28 × 10 cm), and irrigation was carried out to ensure the substrate reached 60 % of its water holding capacity. The evaluations were carried out daily, computing the number of seedlings emerged until the 14th day after the installation of the test, determining the average percentage of seedling emergence for each batch and the seedling emergence speed index, using the method proposed by Maguire (1962).

Electrical conductivity test: electrical conductivity (EC) was determined from the mass system, according to the methodology proposed by the AOSA Vigor Committee (2009). Four replications of 50 seeds were previously weighed on a precision balance (0.001 g); then, the seeds were placed in plastic cups filled with 75 mL of deionized water. The cups were kept for 24 h at 25 °C (Custódio and Marcos Filho, 1997). At the end of this procedure, the reading of the EC of the solution was measured using a Digimed, model DM-32 device. The results were expressed in $\mu\text{S cm}^{-1} \text{g}^{-1}$ of seeds.

Computerized analysis of seedling images: five replications of 20 seeds per lot were used, placed to germinate, and numbered in two rows in the upper third

of the paper towel at 25 °C for 5 d. The substrate was moistened with water equivalent to 2.5 times its mass.

The seedlings were transferred to a sheet of black cardboard to provide the necessary contrast for analysis by the system. Next, the images of the seedlings were scanned using an HP Scanjet 200 scanner, adjusted to a resolution of 100 DPI, and installed in an inverted position inside an aluminum box (60.0 × 50.0 × 12.0 cm) attached to a computer.

The images were analyzed by the software Seed Vigor Imaging System (SVIS) to generate development uniformity and vigor indexes according to Sako et al. (2001), comprising values from 0 to 1000, and seed vigor is directly proportional to these values. After processing the images, mean values of vigor and development uniformity indexes and seedling length (cm) were obtained for each seed batch, as described by Hoffmaster et al. (2003) and Marcos-Filho et al. (2006).

The water content was determined by the oven method at 105 °C (± 3 °C) for 24 h (MAPA, 2009) with two replications of 5 g of seeds for each batch to monitor the moisture content of the seeds during the tests described above. The results were expressed as a percentage (wet basis). This determination was also carried out after performing the accelerated aging test.

Statistical analysis

The results obtained from the analyses of images of seeds and seedlings were submitted to the analysis

of variance (ANOVA) in a completely randomized experimental design, and the means of the batches were grouped by the Scott-Knott test ($p \leq 0.05$). The multivariate analysis, including the principal component analysis (PCA) and the Pearson correlation coefficients (r), was performed for all image parameters obtained from seeds and seedlings, considering individual seeds. The R software was used for the statistical analyses.

Results and Discussion

The free space (Figure 2A) in the internal cavity of rice seeds did not show any statistical difference among the batches. The average seed area (Figure 2B) showed a statistically difference. Relative density (Figure 2C) showed no statistical differences among the batches, considering the averages of the batches.

All parameters obtained from chlorophyll *a* CF images of 620/730 nm (excitation/emission energy) showed statistically differences among the batches. The anthocyanin index (Figure 2D) had the lowest mean value for batch 4 (0.78), while for the chlorophyll index (Figure 2E), the lowest mean value was observed for batch 3 (0.77). The CF (Figure 2F) of seeds from batch 3 had the highest average value (5445.21).

The average reflectance in the 22 wavelengths obtained by the VideomaterLab, showed statistical differences among seed batches (Figure 3), with higher average intensity for batch 3. At the wavelength of 470

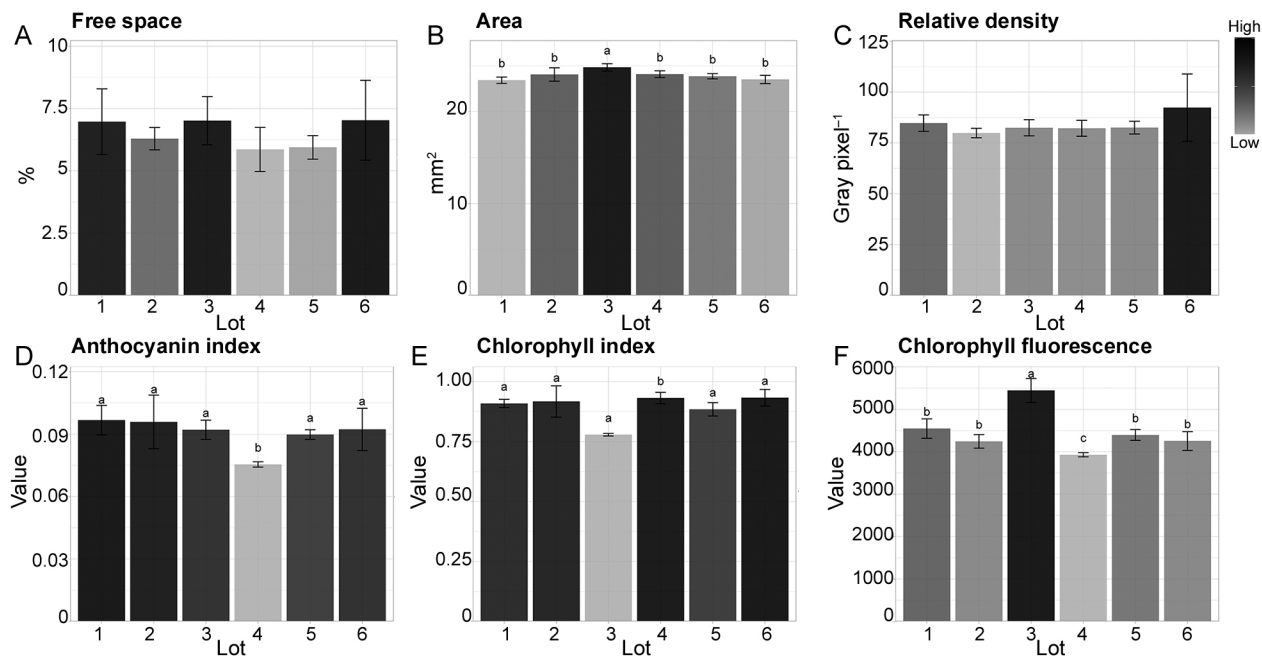


Figure 2 – Variables obtained with X-ray image analysis: free space (A), seed area (B) and relative density (C), anthocyanin index (D), chlorophyll index (E) and chlorophyll fluorescence (F) of seeds from six rice batches. Different letters at the upper ends of the columns, within each evaluation, indicate statistical differences among the batches by Scott-Knott test ($p < 0.05$). The bars represent the standard deviation.

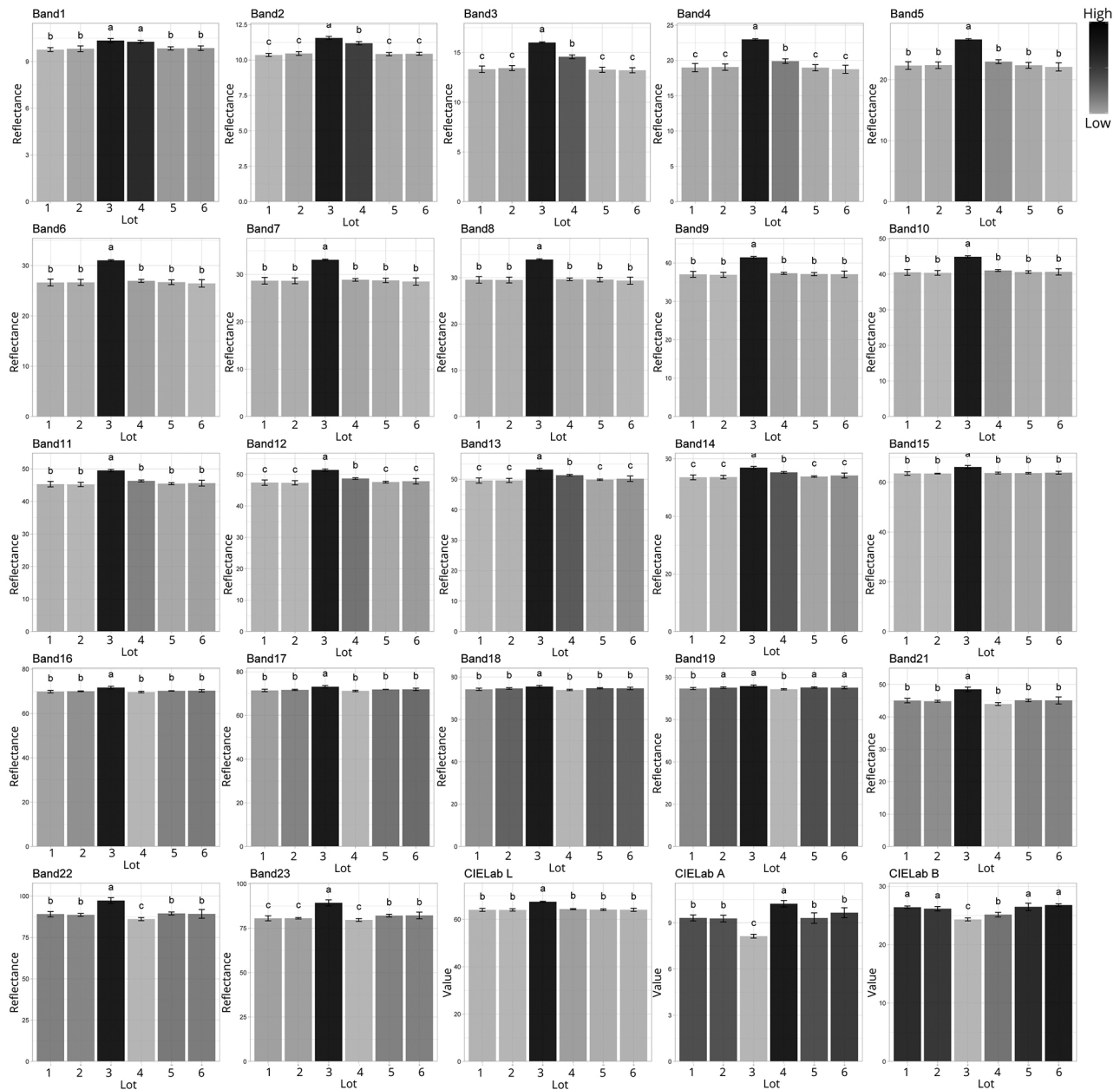


Figure 3 – Multispectral analysis corresponding to 21 spectral bands (Band 1 = 365 nm, Band 2 = 405 nm, Band 3 = 430 nm, Band 4 = 450 nm, Band 5 = 470 nm, Band 6 = 490 nm, Band 7 = 515 nm, Band 8 = 540 nm, Band 9 = 570 nm, Band 10 = 590 nm, Band 11 = 630 nm, Band 12 = 645 nm, Band 13 = 660 nm, Band 14 = 690 nm, Band 15 = 780 nm, Band 16 = 850 nm, Band 17 = 880 nm, Band 18 = 940 nm, Band 19 = 970 nm, Band 21 = 630/700 nm, Band 22 = 645/700 nm, Band 23 = 660/700 nm) of seeds from six rice batches of the BRS Catiana cultivar. Different letters in the upper extremities of the columns, within each evaluation, indicate statistical differences among the batches by the Scott-Knott test ($p < 0.05$). The bars represent the standard deviation.

nm (Band 5), only batch 3 differed from the others, with a higher mean value, while at the wavelengths of 645, 660, and 690 nm (Bands 12, 13, and 14), there was more significant discrimination among the batches.

The CF analysis of 630/700 nm (Band 21), 645/700 nm (Band 22) and 660/700 nm (Band 23) presented

higher values for batch 3, which also had a higher mean value for the CIE Lab L color parameter, but with lower mean values for CIE Lab a* and CIE Lab b*, according to the nCDA model from VideometerLab (Figure 3)

The mean values of the seed batches referring to the quantum yield of the maximum photochemical

efficiency of the FSII (F_v/F_m) and the chlorophyll fluorescence of seedling (CF seedling) at seven, nine, and 11 days after emergence are shown in Figures 4A-C and 4E. These figures show a statistical difference for F_v/F_m among the batches only at nine days after emergence (Figure 4C), while seedling CF differed at nine and 11 days after emergence (Figures 4D and 4F) and did not differ at seven days after emergence (Figure 4B). Furthermore, there was increased CF and photosynthetic efficiency with seedling development.

The germination test (Figure 5A) showed that seeds from batch 2 had the highest average (96 %), followed by seeds from batches 3, 5, and 4 (94 %, 92 %, and 91 %, respectively) with intermediate means and, finally, seeds from batches 6 and 1 (89 % and 85 %, respectively) with the lowest means.

Regarding the vigor tests, the first germination count test showed a better performance for batch 2, followed by batches 5 and 6 (with batch 5 showing a better performance than batch 6) and with lower values for the other batches that performed similarly to each other (Figure 5B).

In the accelerated aging test (Figure 5C) and seedling emergence in the sand (Figure 5E), the seeds from batches 2 and 5 showed higher percentages than the other batches.

For EC (Figure 5D), batches 3 and 1 had the highest values, followed by batches 5, 6, and 2, intermediate values, and batch 4, lowest value.

The evaluation with the SVIS software showed that batch 2 had the greatest total length of seedlings, followed by batches 3, 6, and 4, respectively, with batch 1 showing the shortest length in relation to the others (Figure 5F). The vigor index (Figure 5G) displayed a better performance for batches 2 and 6 compared to the others, which showed similar performance. The development uniformity index showed no difference in performance among the batches (Figure 5H).

The parameters obtained in the analysis of X-ray images (internal free space, seed area, and relative density), considering the average values of the batches, were not related to the germination and vigor tests with any parameter of MSI and CF of the batches of seeds. This is possibly attributed to the fact that the

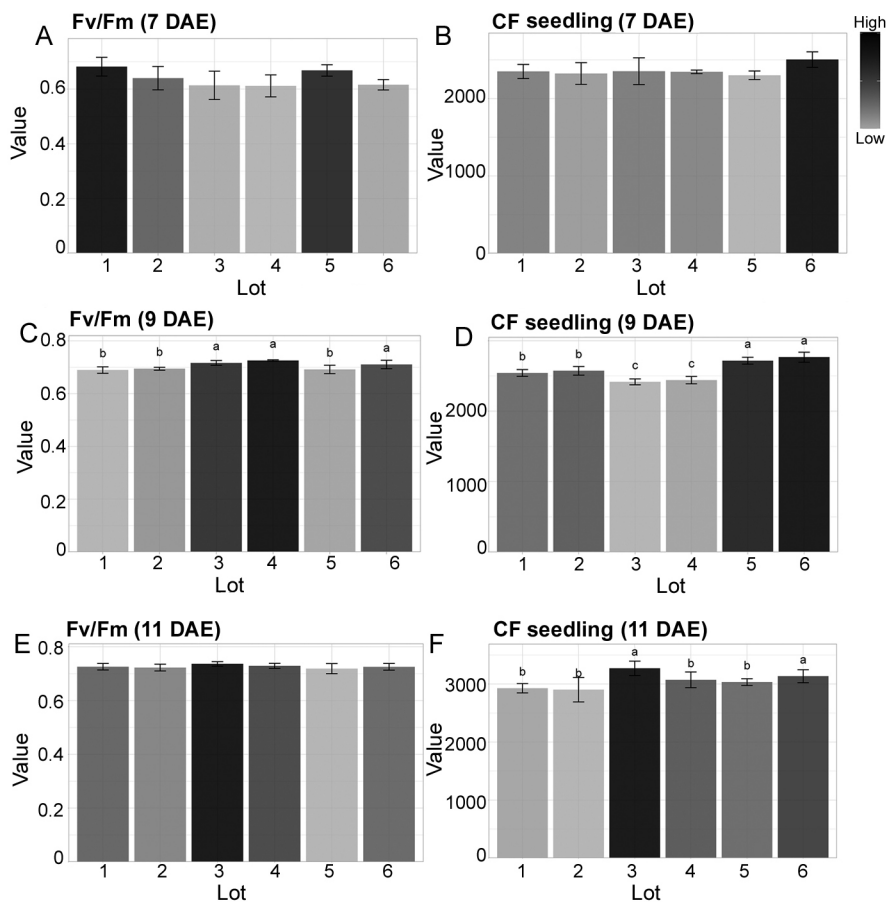


Figure 4 – Quantum yield analyses of the maximum photochemical efficiency of FSII (F_v/F_m) (A, C, E) and chlorophyll fluorescence (CF) of seedlings (B, D, F) at seven, nine, and 11 days after emergence (DAE) from six batches of rice. Different letters in the upper extremities of the columns, within each evaluation, indicate statistical differences among the batches by the Scott-Knott test ($p < 0.05$). The bars represent the standard deviation.

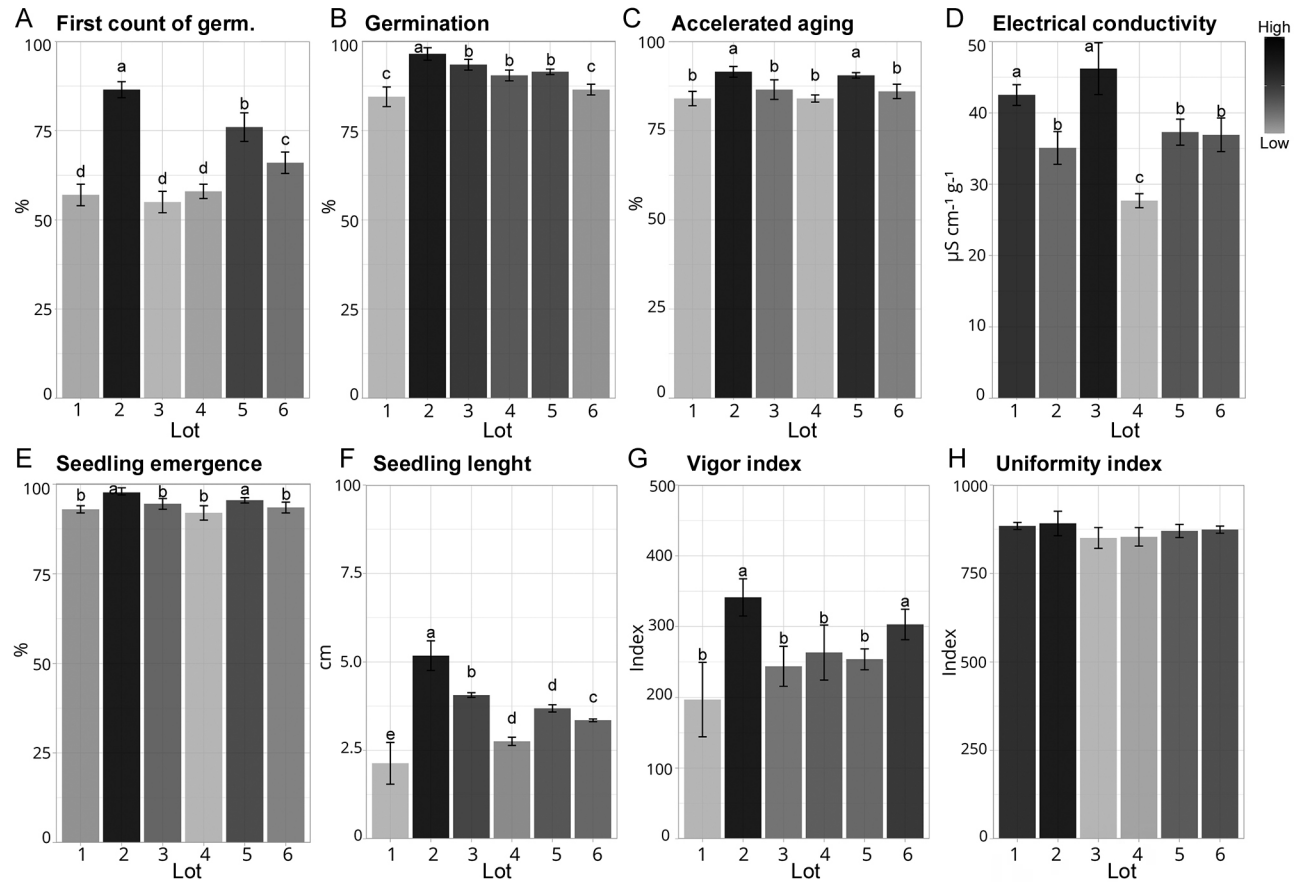


Figure 5 – First count of germination (A), germination (B), accelerated aging (C), electrical conductivity (D), seedling emergence in sand (E), seedling length (F), vigor index (G), development uniformity index (H) of seeds from six batches of rice. Different letters in the upper extremities of the columns, within each evaluation, indicate differences among the batches by the Scott-Knott test ($p < 0.05$). The bars represent the standard deviation.

aforementioned evaluations presented values that were insufficient to compromise the batches evaluated.

The data obtained from the analysis of radiographic, multispectral, and CF images of the seeds, in addition to the F_v/F_m and seedling CF, were subjected to the PCA analysis (Figure 6A). The first two principal components explained 87 % of the total variance between seed and seedling image parameters, with 71 % and 16 % for PC1 and PC2, respectively. This analysis shows the separation of seed batches, with batch 3 presenting higher values of reflectance of the spectral bands and of CF of the seeds and higher values of F_v/F_m and CF of the seedlings at nine and 11 days after emergence.

Correlations were observed between image parameter values (X-ray, multispectral, and chlorophyll fluorescence) of individual seeds and photosynthetic efficiency image parameters (F_v/F_m) and CF of seedlings generated (Figure 6B).

The free space inside rice seeds did not correlate with photosynthetic efficiency (F_v/F_m) and CF of the generated seedlings (Figure 6B). Indeed, when the free space of the seed does not compromise its germination,

the functioning of the photosynthetic apparatus and the seedling chlorophyll concentration are unrelated to the endosperm and the embryo area. Eggplant seeds with larger embryonic areas do not necessarily generate seedlings with greater length (Silva et al., 2012), similar to pepper (Gagliardi and Marcos-Filho, 2011).

Seeds with high mean reflectance in the spectral wavelength bands between 365 nm and 780 nm generated seedlings with higher photosynthetic efficiency (F_v/F_m) 11 days after seedling emergence (Figure 6B). These spectral bands are possibly related to seedling performance.

The reflectance of seeds in the spectral bands from 365 nm to 780 nm also showed a positive correlation with their CF (Figure 6B), suggesting a maintenance of this molecule, reflecting on photosynthetic efficiency (F_v/F_m) of the seedlings generated in seeds with a maximum limit of chlorophyll concentration to germinate.

Soybean seeds subjected to different times of accelerated aging (0 h, 12 h, 24 h, and 48 h) also showed a direct relationship between the CF (365/400 nm) of seeds and the F_v/F_m in the seedlings generated. There

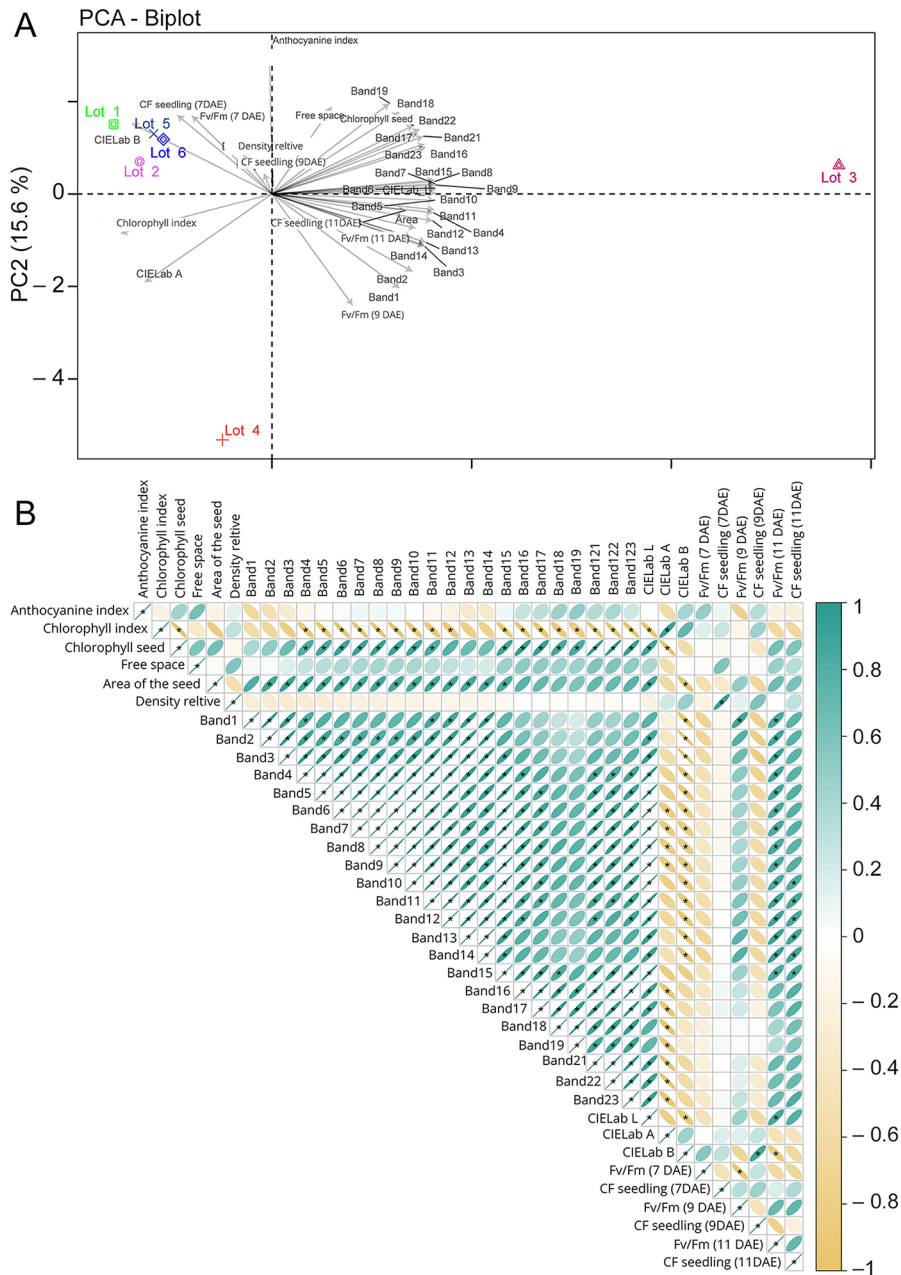


Figure 6 – A) Biplot of the principal component analysis (PCA) obtained from the variables related to X-ray analysis, multispectral, and chlorophyll fluorescence images and seed physiology and quantum yield of FSII photochemical maximum efficiency (F_v/F_m) and chlorophyll fluorescence of plants of six rice seed batches of the cultivar BRS Catiana. PC1 = Principal Component 1; PC2 = Principal Component 2. B) Estimates of Pearson correlations between multiple features of the X-ray analyses, multispectral and chlorophyll fluorescence imaging and physiological analyses of seeds and quantum yield of FSII photochemical maximum efficiency (F_v/F_m) and chlorophyll fluorescence of plants of six rice seed batches of the cultivar BRS Catiana.

was also a more remarkable synthesis of chlorophyll *a* and chlorophyll *b* in seeds aged 48 h and a greater accumulation of chlorophyll *a* in seedlings from the chlorophyll index (Silva et al., 2021).

The data suggest a possible compensatory mechanism during seedling development to overcome

the secondary effects of undegraded chlorophyll at high concentrations in the initial phase of germination. Such mechanism may be related to a larger amount of chlorophyll *a* in seedlings to improve the conversion of solar radiation into chemical energy, reflecting on the photochemical activity of photosystem II (F_v/F_m).

The quantum yield of the maximum photochemical efficiency of PSII, given by: F_v/F_m ($F_v = F_m - F_0$) is typically measured on an intact leaf from a dark adaptation for 20 min prior to determination. A saturating flash is focused on the leaf surface, causing the fluorescence to increase from the basal state (F_0) to its maximum value (F_m). Thus, the first electron acceptor of PSII, Quinone A, is totally reduced. F_v/F_m is around 0.8 in healthy leaves, regardless of the plant species. A lower value indicates that the PSII reaction centers are damaged, a phenomenon called photo-inhibition (Schreiber and Bilger, 1993). Thus, in germinated rice seeds, the chlorophyll content measured using the CF imaging technique positively affected the photosynthetic potential of the generated seedling, with a possible contribution from the chlorophyll molecules in the seed in the photosynthetic apparatus.

Based on the nCDA model, seeds with high CIELab L and low CIELab b* values generated seedlings with greater photosynthetic efficiency (F_v/F_m) 11 days after seedling emergence (Figure 6B). This parameter allows the reduction of the spectral data dimensionality of all wavelengths obtained, resulting in linear combinations of these features, called canonical variables, which allow the capture of the simultaneous effect of the reflectance values of the spectral bands as well as variations not perceived when used of original features individually (Khattri and Naik, 2000).

Seed 1 generated a seedling with high photosynthetic capacity 11 days after emergence, indicated by the high F_v/F_m value of 0.777 (Figure 7H), in addition to presenting a high CF value of 34090 (Figure 7G). This seed showed mean fluorescence values of chlorophyll a of 645/700 nm of 90.12 (Figure 7B), chlorophyll b of 660/700 nm of 84.15 (Figure 7C), chlorophyll a of 620/730 nm of 34234 (Figure 7D) and with a reflectance pattern following high values at wavelengths from 365 nm to 780 nm (Figure 7E).

Seed 2 presented mean fluorescence values of chlorophyll a at 645/700 nm of 88.72 (Figure 7J), chlorophyll b at 660/700 nm of 79.81 (Figure 7K) and chlorophyll a at 620/730 nm of 42.34 (Figure 7L), values lower than those observed for seed 1. This distinction was also observed for the reflectance pattern, which showed low values at wavelengths between 365 nm and 780 nm (Figure 7M). The seedling generated from seed 2 had low photosynthetic capacity 11 days after emergence, indicated by the low F_v/F_m value of 0.526 (Figure 7O), in addition to having a low CF value of 31889 (Figure 7P). In addition, the RBB images of the seeds and seedlings generated, respectively, are shown in Figures 7A-F (seed 1) and 7I-N (seed 2).

Thus, CF imaging using different combinations of excitation emission, combined with MSI, has high accuracy to distinguish seeds that generate plants with different light conversion capabilities in the chemical photosynthesis processes. Considering the growing demand of the agricultural industry for technologies to

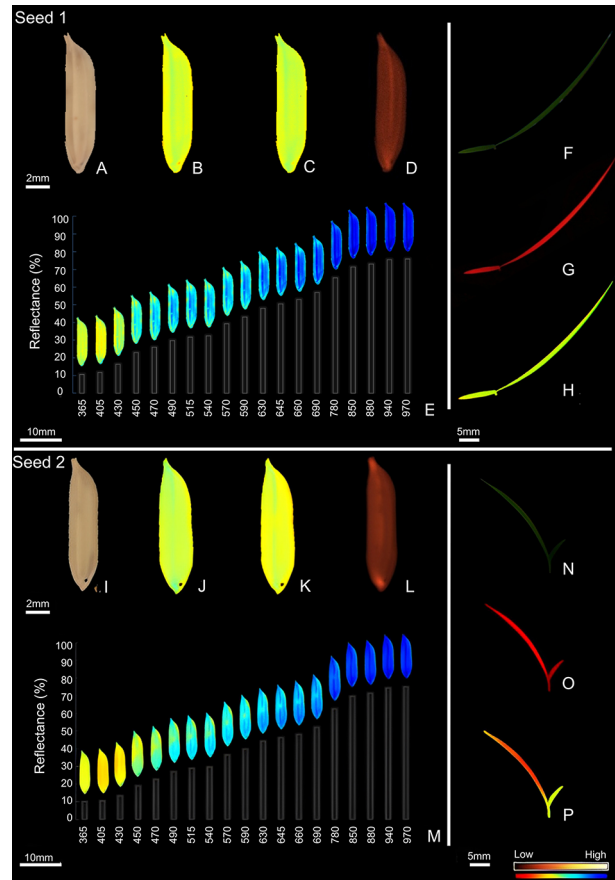


Figure 7 – RGB images (A and I), of chlorophyll a fluorescence at 620/730 nm (B and J), of chlorophyll a fluorescence at 645/700 nm (C and K), of chlorophyll b fluorescence at 660/700 nm (D and L) and of 19 spectral bands using the “Inverse jet” filter (VideometerLab4® software) with respective reflectance histogram (E and M) of rice seed, with the RGB images (F and N), of chlorophyll fluorescence (G and O) and of photosynthetic efficiency measured by F_v/F_m (H and P) of the seedling originated at 11 days after emergence.

improve the efficiency of production processes, these new technologies emerge as important alternatives in rice seed quality control programs.

It can therefore be concluded that the higher photosynthetic efficiency of rice seedlings at 11 days after emergence is directly related to the reflectance between 365 nm and 780 nm spectral bands of the seeds.

Acknowledgments

To the Conselho Nacional de Desenvolvimento Científico e Tecnológico (CNPq), for granting a scholarship to the first author. To the Fundação de Amparo à Pesquisa do Estado de São Paulo (FAPESP), for the availability of the VideometerLab, SeedReporter and MultiFocus Radiography System equipment, linked to the Young Researcher in Emerging Centers Project - Process 2017/15220-7.

Authors' Contributions

Conceptualization: Silva AS, Cicero SM. **Data acquisition:** Silva AS. **Data analysis:** Silva AS. **Design of methodology:** Silva AS, Cicero SM, Gomes Junior FG. **Writing – original draft:** Silva AS. **Writing – review & editing:** Cicero SM, Gomes Junior FG.

References

- Association of Official Seed Analysts [AOSA]. 2009. Seed Vigor Testing Handbook. AOSA, Springfield, MA, USA (Contribution, 32).
- Ashraf M, Harris PJC. 2013. Photosynthesis under stressful environments: An overview. *Photosynthetica* 51: 163-190. <https://doi.org/10.1007/s11099-013-0021-6>
- Boelt B, Shrestha S, Salimi Z, Jørgensen JR, Nicolaisen M, Carstensen JM. 2018. Multispectral imaging: a new tool in seed quality assessment? *Seed Science Research* 28: 222-228. <https://doi.org/10.1017/S0960258518000235>
- Custódio CC, Marcos Filho J. 1997. Potassium leachate test for the evaluation of soybean seed physiological quality. *Seed Science and Technology* 25: 549-564.
- Gagliardi B, Marcos-Filho J. 2011. Relationship between germination and bell pepper seed structure assessed by the X-ray test. *Scientia Agricola* 68: 411-416. <https://doi.org/10.1590/S0103-90162011000400004>
- Gitelson AA, Gritz Y, Merzlyak MN. 2003. Relationships between leaf chlorophyll content and spectral reflectance and algorithms for non-destructive chlorophyll assessment in higher plant leaves. *Journal of Plant Physiology* 160: 271-282. <https://doi.org/10.1078/0176-1617-00887>
- Hoffmaster AL, Fujimura K, McDonald MB, Bennett MA. 2003. An automated system for vigor testing three-day old soybean seedlings. *Seed Science and Technology* 31: 701-713. <https://doi.org/10.15258/sst.2003.31.3.19>
- Khattree R, Naik DN. 2000. *Multivariate Data Reduction and Discrimination with SAS® Software*. SAS Institute, North Carolina, p. 559.
- Maguire JD. 1962. Speed of germination and in selection and evaluation for seedling emergence and vigor. *Crop Science* 2: 176-177. <http://dx.doi.org/10.2135/cropsci1962.0011183X00020020033x>
- Marcos-Filho J, Bennett MA, McDonald MB, Evans AF, Grassbaugh EM. 2006. Assessment of melon seed vigour by an automated computer imaging system compared to traditional procedures. *Seed Science and Technology* 34: 485-497. <https://doi.org/10.15258/sst.2006.34.2.23>
- Mastrangelo T, França-Silva F, Mascarin GM, Silva CB. 2019. Multispectral imaging for quality control of laboratory-reared *Anastrepha fraterculus* (Diptera: Tephritidae) pupae. *Journal of Applied Entomology* 143: 1072-1079. <https://doi.org/10.1111/jen.12716>
- Mathur S, Agrawal D, Jajoo A. 2014. Photosynthesis: Response to high temperature stress. *Journal of Photochemistry and Photobiology B: Biology* 137: 116-126. <https://doi.org/10.1016/j.jphotobiol.2014.01.010>
- Ministério da Agricultura, Pecuária e Abastecimento [MAPA]. 2009. Rules for Seed Analysis = Regras de análise de sementes. MAPA, Brasília, DF, Brazil (in Portuguese).
- Olesen MH, Carstensen JM, Boelt B. 2011. Multispectral imaging as a potential tool for seed health testing of spinach (*Spinacia oleracea* L.). *Seed Science and Technology* 39: 140-150. <https://doi.org/10.15258/sst.2011.39.1.12>
- Ooms D, Destain MS. 2011. Evaluation of chicory seeds maturity by chlorophyll fluorescence imaging. *Biosystems Engineering* 110: 168-177. <https://doi.org/10.1016/j.biosystemseng.2011.07.012>
- Sako Y, McDonald MB, Fujimura K, Evans AF, Bennett MA. 2001. A system for automated seed vigor assessment. *Seed Science and Technology* 29: 625-636.
- Schreiber U, Bilger W. 1993. Progress in chlorophyll fluorescence research: major developments during the past years in retrospect. p. 151-173. In: Behnke HD, Lüttge U, Esser K, Kadereit JW, Runge M. eds. *Progress Botany*. Springer, Berlin, Germany. https://doi.org/10.1007/978-3-642-78020-2_8
- Shrestha S, Deleuran LC, Olesen MH, Gislum R. 2015. Use of multispectral imaging in varietal identification of tomato. *Sensors* 15: 4496-4512. <https://doi.org/10.3390/s150204496>
- Silva CB, Lopes MM, Marcos-Filho J, Vieira RD. 2012. Automated system of seedling image analysis (SVIS) and electrical conductivity to assess sun hemp seed vigor. *Revista Brasileira de Sementes* 34: 55-60. <https://doi.org/10.1590/S0101-31222012000100007>
- Silva VN, Sarmento MB, Silveira AC, Silva CS, Cicero SM. 2013. *Acca sellowiana* O. Berg seed morphology evaluation by image analysis. *Revista Brasileira de Fruticultura* 35: 1158-1169 (in Portuguese, with abstract in English). <https://doi.org/10.1590/S0100-29452013000400027>
- Silva CB, Oliveira NM, Carvalho MEA, Medeiros AD, Nogueira ML, Reis AR. 2021. Autofluorescence-spectral imaging as an innovative method for rapid, non-destructive and reliable assessing of soybean seed quality. *Scientific Reports* 11: 17834. <https://doi.org/10.1038/s41598-021-97223-5>
- Silva AS, Cicero SM, Silva FF, Gomes-Junior FG. 2023. X-ray, multispectral and chlorophyll fluorescence images: innovative methods for evaluating the physiological potential of rice seeds. *Journal of Seed Science* 45. <https://doi.org/10.1590/2317-1545v45257617>
- Schneider CA, Rasband WS, Eliceiri KW. 2012. NIH Image to ImageJ: 25 years of image analysis. *Nature Methods* 9: 671-675. <https://doi.org/10.1038/nmeth.2089>
- Smolikova G, Dolgikh E, Vikhnina M, Frolov A, Medvedev S. 2017. Genetic and hormonal regulation of chlorophyll degradation during maturation of seeds with green embryos. *International Journal of Molecular Sciences* 18: 1-15. <https://doi.org/10.3390/ijms18091993>
- Smolikova G, Shiroglazova O, Vinogradova G, Leppyanen I, Dinastiya E, Yakovleva O, et al. 2020. Comparative analysis of the plastid conversion, photochemical activity, and chlorophyll degradation in developing embryos of green-seeded and yellow-seeded pea (*Pisum sativum*) cultivars. *Functional Plant Biology* 47: 409-424. <https://doi.org/10.1071/FP19270>